FLIGHT PERFORMANCE ESTIMATION FOR EVTOL QUADCOPTER CONFIGURATIONS

Maksim Miasnikov, mmyasnikov@mi-helicopter.ru
Sergey Esaulov, sergey_esaulov@bk.ru
Igor Ilyin, irilyin@mi-helicopter.ru
National Helicopter Center Mil&Kamov (Russia)

Abstract

The present study attempts to compare flight performance of the most popular eVTOL (electrical Vertical Take-Off and Landing) aerodynamic configurations of our days. This study gives a theoretical evaluation of the possible VTOL design of different configurations with full electric or hybrid power plant aimed at the urban mobility applications. Conventional rotorcraft, quadcopters, tiltrotor and tiltwing aircrafts with open rotors and ducted fans have been considered. Different eVTOL design available structural elements mass distributions were found. Flight performance of the eVTOL with full electric and hybrid power plants is estimated. Power available and required for speed envelope from hover to maximal speed modes are calculated. Optimal specific parameters of fully electric and hybrid power plant elements (batteries, generators, electric motors, etc.) are defined to provide acceptable eVTOL flight performance.

1. INTRODUCTION

The forecast analysis reveals that urban traffic has to become more complicated for the next few years and the number of megalopolises is growing up. At the same time, the quality of life in such areas is expected to continually degrade. As a result, the necessity arose to dramatically decrease traffic overloading and to minimize environmental pollution. It appears the brand new mobile concept including absolutely new background and new traffic idea that presumes both upgraded infrastructure and new mobile approach.

Today, one of the most promising ways of air vehicle evolution is an eVTOL (electric Vertical Take-Off and Landing) concept. Electrically driven VTOL features higher efficiency, environmental security and cheaper life cycle expenses. New eVTOL design needs to be globally revised in terms of VTOL main systems architecture.

This enthusiasm is stimulated on one hand by automobile electric engine evolution (and recently applied in aviation as well) and on the other hand by increasing number of the ground traffic problems induced by growing number of ground vehicles.

Development and improvement of the small unmanned aerial vehicles (SUAV) equipped mainly with electric power engines has become perceivable impulse to eVTOL evolution.

Essential difference in power efficiency of conventional hydrocarbon fuel and electrochemical battery (12000 W·h/kg versus 150-200 W·h/kg) forces eVTOL designers to foresee many different aerodynamic solutions in order to minimize power consumption. That makes understandable extremely wide variety of eVTOL concepts and designs.

The present study attempts to compare flight performance of eVTOL featuring the most popular aerodynamic configurations of our days. This research deals with multirotor design using several rotors driven by electric motors. It means rotors may be open, or in ducted fans, single or coaxial. It should be emphasized that multirotor VTOLs have design features that are fundamentally discrepant of conventional helicopters.

The present study provides a theoretical evaluation of the possible VTOL design with fully electric or series hybrid power plant configurations that are comparable to the light helicopter class.

Presented at 47th European Rotorcraft Forum, United Kingdom, 7-9th September, 2021

There have been worked out flight performance mathematical models for the following VTOL configurations:

- Conventional helicopter with one main rotor and one tail rotor. This configuration included design with electrically driven main rotor and tail rotor with mechanical transmission (Fig.1).
- Quadcopter with 4 X-type open rotors (Fig. 2a).
- Quadcopter with 4 X-type ducted fans (Fig. 2b).
- Quadcopter with aerodynamic lifting surfaces and open tilt rotors (Fig. 3a, b).
- Quadcopter with aerodynamic lifting surfaces and tilt ducted fans.
- Quadcopter with tilt wings and open rotors.
- Quadcopter with tilt wings and ducted fans (Fig. 3c, d).

As a result of calculations done, different eVTOL design available structural elements mass distributions were found. There were defined range and endurance of VTOL with full electric and hybrid power plant at the level flight mode. Available and required power for vertical, level, and transient (for tiltrotors and tiltwings) flight modes were calculated. Some output results dealt with the first five VTOL design configurations were revealed in [1, 2].

Flight performance of the above VTOL configurations was estimated in order to compare their efficiency. All calculations based on momentum theory methods accepted possible adjustments depending on outcome of experiment. There was considered VTOL aircrafts with fixed payload. Structural elements masses were chosen with a certain degree of approximation based on the open sources data.

Obtained results might be taken as the first approximation for the further studies related with exploring of the future eVTOL concepts to be applied as urban airtaxi.

2. MATHEMATICAL MODEL OF THE eVTOL CONCEPT WITH HYBRID OR FULL ELECTRIC POWER PLANT

Mathematical model of the eVTOL concept is based on flight vehicle mass balance equation as follows:

$$(1)\ m_0\left(1-\sum_{i=1}^{n}\overline{m}_i\right)=Pn_{MR}k_p\left(\frac{1}{\overline{P}_{EM}}+\frac{1}{\overline{P}_{gen}}+\frac{1}{\overline{P}_{HE}}+\overline{m}_{inv}\right)+\sum_{i=1}^{n}m_i+\overline{m}_{bat}Pn_{MR}t_{end},$$

$$\sum_{i=1}^{n}\overline{m}_i=\overline{m}_{rs}+\overline{m}_{fus}+\overline{m}_{ue}+\overline{m}_{ae}+\overline{m}_{ew}+\overline{m}_{HE},$$

$$\sum_{i=1}^{n}m_i=m_f+m_{trans}+m_{FC}+m_{FS}+m_{OS}+m_{Ch}+m_{PL}+m_{cr}+m_{TR}+m_{WG},$$

where P – thrust engine power in hover mode, $k_p \geq 1$ – power plant safety factor, m_{PL} – mass of the payload, m_{cr} – crew personnel mass, t_{end} – hover endurance based on battery, m_0 – flight vehicle mass, m_{WG} – wing mass, $\bar{P}_{HE}$ – heat engine (*ICE or GTE*) specific power, n_{MR} – number of main rotors.

Equation (1) is universal for all types of eVTOL being considered in the study, with both full electric and hybrid power plant. In general, equation (1) is nonlinear as relating to P and its solution can be obtained only by numerical methods.

2.1. Aerodynamic prediction for multirotor VTOL with open rotors and conventional single-rotor helicopter

According to the momentum theory [3, 4] open rotor thrust in hover mode can be evaluated with the reasonable for an initial estimate accuracy by formula

$$(2)\qquad T=(2\rho F_{MR}P^2)^{1/3},$$

where ρ – air density, $F_{MR}=0.25\pi D_{MR}^2$ – rotor disk area, D_{MR} – main rotor diameter, P – thrust motor power.

Rearranging expression (2) and taking into account coefficients η, ξ and χ we will get the following:

$$(3)\qquad T=\left(P\xi\eta\sqrt{2\rho F_{MR}\chi}\right)^{2/3},$$

where ξ – mechanical transmission loss factor due to cooling and torque compensation, η – main rotor figure of merit – ratio of the ideal induced power to the total rotor power, P – power plant output, χ – ratio of the effective rotor disk area contributing to thrust generation to the total disk area F_{MR}.

Equating formula (3) to the flight vehicle weight $T = G = m_0 g$, we will get the flight vehicle mass expression:

(4) $$m_0 = \frac{1}{g}\left(N\xi\eta\sqrt{2\rho F_{MR}\chi}\right)^{2/3},$$

where g – gravitational acceleration.

Substituting expression (4) in equation (1) we get nonlinear relating to P equation for the hover mode.

(5) $$\frac{n_{MR}}{g}\left(P\xi\eta\sqrt{2\rho F_{MR}\chi}\right)^{2/3}(1 - \bar{m}_{rs} - \bar{m}_a - \bar{m}_{ue} - \bar{m}_{ae} - \bar{m}_{ew} - \bar{m}_{HE}) - Pn_{MR}k_p\left(\frac{1}{\bar{P}_{EM}} - \frac{1}{\bar{P}_{gen}} - \frac{1}{\bar{P}_{EM}}(1-\xi) - \frac{1}{\bar{P}_{HE}} - \bar{m}_{inv}\right) - \bar{m}_{bat}Pn_{MR}t_{end} - m_f - m_{trans} - m_{FC} - m_{fs} - m_{os} - m_{Ch} - m_{PL} - m_{TR} - m_{cr} - m_{WG} = 0$$

Analytic solution of the equation (5) is too intricate, therefore numerical solution has been found.

To calculate the induced power of the free rotor in edgewise rotor flow mode we used the Glauert theory [3, 4]. It was assumed that the main rotor blown by the oncoming flow with velocity V and the angle of attack α.

Let us introduce velocity normalized components – parallel and normal to rotor disk. These components are called rotor advance ratio μ and inflow ratio λ respectively, and they are defined by the following formulae

(6) $$\mu = \frac{V\cos\alpha}{\Omega R},\ \lambda = \frac{V\sin\alpha + v}{\Omega R} = \mu\tan\alpha + \lambda_i,$$

where induced velocity presented as induced inflow ratio

(7) $$\lambda_i = \frac{C_T}{2\sqrt{\mu^2+\lambda^2}}$$

Inflow ratio λ can be found from the solution of the equation

(8) $$\lambda - \mu\tan\alpha - C_T/\left(2\sqrt{\mu^2+\lambda^2}\right) = 0$$

For each rotor, thrust coefficient C_T is defined by the formula

(9) $$C_T = \frac{T}{\rho F_{MR}(\Omega R)^2}$$

Main rotor thrust in (9) can be calculated as follows

(10) $$T = G/(n_{MR}\cos\alpha)$$

Formula (10) is fair for any type of VTOL with open rotors on the assumption with the rotor angle of attack absolute value approximately equals to the pitch trim angle.

In addition, we have to assume that aerodynamic interference between thrust rotors offset enough from each other is a little one and can be taken into account by entering special factors to the induced power [4]. In case of the light VTOL with offset open rotors without overlapping or ducted fans it is admissible for provisional estimate.

In the present study main rotors thrust values for all types of chosen VTOL within all flight mode envelopes were defined by getting solution for the flight vehicle trim equations.

Power required for VTOL cruise flight can be represented in the sum of induced power, blade profile drag, wave power and parasite drag:

(11) $$P = P_i + P_0 + P_w + P_p\ ,$$

or going to power factors

(12) $$C_P = C_{Pi} + C_{P_0} + C_{P_w} + C_{P_p}$$

Coefficients in (12) might be calculated as following:

(13) $$C_{Pi} = P_i/\rho F_{MR}(\Omega R)^3 = Tv/\rho F_{\mathrm{MR}}(\Omega R)^3,$$

(14) $$C_{P_0} = \sigma c_{d_0}(1 + 4.6\mu^2)/8\ ,$$

(15) $$C_{P_w} \approx K_c(M_0 - 0.4)^2,$$

where K_c – compressibility factor, depending on aerodynamic configuration, geometric twist and blades finishing, main rotor thrust coefficient and VTOL velocity.

(16) $$C_{P_p} = DV/\rho F_{MR}(\Omega R)^3$$

Then power required P will be defined as follows:

(17) $$P = C_P\rho F_{MR}(\Omega R)^3$$

Consequently, required rotor torque may be evaluated as following

(18) $$M = P/\Omega\ .$$

2.2. Aerodynamic prediction for multirotor VTOL with ducted fans

We used momentum theory to calculate ducted fan thrust as well [5]. According to this theory, ducted fan thrust may be represented in the sum of rotor thrust and duct thrust form

(19) $$T = T_D + T_R$$

Expression (19) is handier to use in dimensionless form relative to summarized ducted fan thrust T

(20) $$\overline{T}_D + \overline{T}_R = 1$$

Summarized ducted fan thrust in hover mode might be calculated as follows

(21) $$T = K\left(\sqrt{2\rho\pi R^2}\eta_0 P\right)^{2/3},$$

where K – quality index of the ducted fan system

(22) $$K = \sqrt[3]{k_V/2\overline{T}_{R0}^2},$$

(23) $$k_V = V_2/V_1 = 1/n\,,$$

(24) $$\overline{T}_{D0} = \frac{1}{2k_V}(k_V^2 + \xi_k),$$

n – diffuser area ratio, $V_1 = V + v_1$ – inflow rate in rotor disk plane, $V_2 = V + v_2$ – total velocity in outgoing flow, V – undisturbed airflow velocity, ξ_k– aggregate coefficient of local drag, P – ducted fan required power in hover mode

(25) $$\xi_k = \xi_c + \xi_d + \xi_o,$$

ξ_c – duct inlet loss, ξ_d – diffuser loss, ξ_o – other internals loss.

For the ducted fan thrust calculation in axial flow mode we might assume that undisturbed airflow runs towards ducted fan axis with velocity V.

Expression for the relative ducted fan thrust might be represented as following [5]:

(26) $$\overline{T}_R = \frac{\overline{T}_{R0} - \frac{\widehat{V}}{2k_V}\left[\xi_c(2-\widehat{V}) + k_V^2\widehat{V}\right]}{1-\widehat{V}},$$

where $\overline{T}_{R0}$ – relative rotor thrust in hover mode,

(27) $$\widehat{V} = 2\Big/\left(1 + \sqrt{1 + \frac{4Tk_V}{\rho F_{MR}V^2}}\right)$$

Ducted fan power would be defined as:

(28) $$P = T_R V_1\,,$$

where V_1 – inflow rate in rotor disk plane.

Let us introduce dimensionless velocity $\tilde{V}_1 = V_1/v_{10}$, where $v_{10} = \sqrt{T/\rho k_V F_{MR}}$ – rate of flow through disk area in hover mode.

In case of axial flow, expression for $\tilde{V}_1$ can be obtained using momentum equation to airflow ingoing along an axis of the ducted fan.

(29) $$T = m(V_2 - V) = m(k_V V_1 - V);$$
$$m = \rho F_{MR} V_1 = \rho F_{MR} V_2/k_V$$

Evaluating V_1 from (29) and relating all velocities to v_{10} we will get:

(30) $$\tilde{V}_1 = \left(\tilde{V} + \sqrt{\tilde{V}^2 + 4k_V^2}\right)/2k_V$$

As it was shown in [5] all expressions, we have taken above, can be used in case of edgewise flow. Such a mode is typical for VTOL having rotor system with ducted fans fixed relative to flight vehicle airframe in cruise flight mode and during climb or descent. For tiltrotors and tiltwings edgewise flow is typical in transitional flight.

Therefore, aerodynamic prediction of the ducted fan in edgewise mode is similar to that of the axial flow mode with specific velocity component $V_y = V\sin\alpha$. However, it should be noted that application of the above algorithm for edgewise flow mode is admissible if the duct length is quite enough for the airflow flowing through the fan to lose completely its horizontal velocity component and diffusor output flow is in the form of fully expanded axial flow with slipstream pressure equals to atmospheric one.

2.3. Aerodynamic prediction of the wing for tilted rotor quadcopter eVTOL

Aerodynamic prediction of the lifting surface for convertible flight vehicles with 4 tilted rotors (Fig. 3) was done analytically using methodology provided in the reference [6]. Using a rectangular wing for the light convertible VTOL is the most reasonable choice in terms of simplicity of calculation and design.

Finite-span wing lift coefficient on linear section of the angle of attack function may be calculated as following:

(31) $C_L = C_{L0} + (dC_L/d\alpha)\alpha,$

where C_{L0} – wing lift coefficient at $\alpha = 0$, $dC_L/d\alpha$ – lift curve slope.

(32) $dC_L/d\alpha = a_0/[1 + (57.3a_0/e\pi AR)] = a$

Taking into account (32), expression (31) will take a look:

(33) $C_L = \frac{1}{1+(57.3a_0/e\pi AR)}(C_{l0} + a_0\alpha),$

where C_{l0} and a_0 – lift coefficient and lift curve slope respectively for two-dimensional airfoil, $e \leq 1$ – Oswald coefficient, considering difference between finite-span wing distribution of circulation and elliptical one, AR – wing aspect ratio. We have chosen NACA 2412 as a main airfoil profile, which is widely used for light airplane wings.

Finite-span wing aerodynamic drag factor can be represented as follows:

(34) $C_D = C_{DP} + C_{Di} + C_{Dw},$

where C_{DP} – wing parasite drag coefficient, C_{Di} – induced drag coefficient, C_{Dw} – wave-drag coefficient.

When considering light eVTOL, typified by the low-speed flight, C_{Dw} coefficient might be omitted. Induced drag coefficient can be found as following:

(35) $C_{Di} = C_L^2/e\pi AR$

Wing airfoil parasite drag coefficient might be approximated as following:

(36) $C_d = C_{d0} + kC_l^2$,

where C_{d0} – airfoil zero-lift drag coefficient, k – dimensionless coefficient.

2.4. Rotor trim tilt angle calculation for quadcopter eVTOL with tilt rotors in conversion mode

To analyze required rotor trim tilt angle δ (Fig. 4a) for the tiltrotor of quadcopter type in conversion mode, let us write force equilibrium equations in wind axis:

(37) $n_{MR}T\cos(\alpha + \delta) - X_a(\alpha, \delta) - G\sin\gamma = 0$

(38) $n_{MR}T\sin(\alpha + \delta) + Y_a(\alpha, \delta) - G\cos\gamma = 0$,

where T – rotor thrust, G – VTOL take-off weight, α – VTOL angle of attack, γ – flight-path angle, $X_a(\alpha, \delta)$, $Y_a(\alpha, \delta)$ – VTOL drag and lift forces respectively.

2.5. Rotor trim tilt angle calculation for quadcopter eVTOL with tilt wings in conversion mode

In case of quadcopter vehicle with tilted wings, force equilibrium equations look the same as equations (37) and (38). However, aerodynamic forces calculations in conversion mode would be a little bit complicated. Wing of such vehicles operates at great angles of attack (Fig. 4b) and requires flap system and/or boundary layer active control system.

Airflow rate near tilt wing might be represented as resultant vector sum of free-stream velocity and rotor induced velocity:

(39) $V_\Sigma = \sqrt{V_\infty^2 + V_{ind}^2 + 2V_\infty V_{ind}\cos(\alpha + \delta + \alpha_0)};$

Wing angle of attack with respect to slipstream can be calculated as follows:

(40) $\alpha_{wing} = \sin^{-1}\left(\frac{V_\infty}{V_\Sigma}\sin(\alpha + \delta + \alpha_0)\right).$

In particular case, when $V_{ind} \ll V_\infty$ and $V_\infty/V_\Sigma \to 1$, angle α_{wing} is just a sum of the tilt wing quadcopter angle of attack, tilt wing deflection angle and rotor axis incidence towards wing chord.

(41) $\alpha_{wing} = \alpha + \delta + \alpha_0.$

Flap system operation consequence might be as following:

- within the airspeed range from 0 till 50 km/h flaps deflection angle increases from 0° (or any other start point resulted from trim

parameters of flight vehicle at hover mode) till 40° according to linear law;
- within the airspeed range from 50 till 75 km/h flaps deflection angle is constant and maximal of 40°;
- within the airspeed range from 75 till 200 km/h flaps deflection angle decreases from 40° till 0° according to linear law.

The airspeed ranges and deflection angles above may considerably change depending on the wing airfoil and existence of the boundary layer active control system.

3. DIFFERENT eVTOL AERODYNAMIC CONFIGURATION PREDICTED RESULTS

Initial data for eVTOL performance prediction with fully electric power plant and hybrid power plant are represented in Table 1 and Table 2 respectively.

Specific mass parameters for thrust electric motors, generators, batteries, inverters, diesel and gas turbine power plants available presently were chosen based on information provided by open sources and papers [7, 8].

Performance prediction was done for two types of power plant: 1) hybrid power plant with heat engine and batteries allowing hover for 5 min, 2) fully electric power plant. The reason of the diesel engine application in hybrid power plant is due to its best fuel consumption efficiency among other types of internal combustion engines. Structural elements mass distribution of the eVTOL resulting from aerodynamic prediction related to take-off mass (to m_0) for different types of power plants is represented in Tables 3 and 4. Mass distributions in relative values for all considering eVTOL are shown on Figure 5-8.

Functionality obtained shows that the main contribution to the flight vehicle mass with hybrid power plant comes from the fuselage structure mass components and internal combustion engine. Moreover, for a single rotor helicopter fuselage structure mass contribution prevails.

This can be explained by less required power that helicopter power plant employs in comparison with quadcopters.

In case of fully electric power plant the main contribution to the eVTOL take-off mass comes from batteries. Their mass reaches 28.5 % of MTOW for a single rotor helicopter.

Maximal mass contribution of 39.5 % to the vehicle mass comes from batteries of the ducted fan quadcopter. In case of open rotors quadcopter, it reaches 38.4%. Single rotor helicopter with both types of power plant has obvious load factor advantage (10.6 – 11.7%). The least load factor value belongs to quadcopter with ducted fans (8.6 – 8.7 %).

Having done structure elements mass distribution computation, analytical prediction of the eVTOL flight performance was accomplished.

Hybrid power plant eVTOL flight range and endurance are defined by fuel range that can be defined by formulae (42), (43), employed for the flight vehicles with conventional power plant performance calculation.

(42) $$L = \int_{m_1}^{m_0} \frac{dm}{q_r},$$

(43) $$t = \int_{m_1}^{m_0} \frac{dm}{q_h},$$

where m_0 and m_1 – eVTOL mass in the beginning and at the end of the level-flight segment for which computation is done. If cargo is not dropped, eVTOL mass change equals to fuel consumption at level-flight leg:

$$m_f = m_0 - m_1$$

Hourly and range fuel consumption q_h and q_r for eVTOL can be expressed via engine specific fuel consumption C_e and engine required power *P*:

(44) $$q_h = C_e P,\ q_r = \frac{C_e P}{3.6V}$$

Approximate range and endurance calculation for eVTOL with fully electric power plant can be done as following:

(45) $$t = \frac{Q}{P},\ L = 3.6Vt$$

Output obtained by formula (45) will be upper estimate as the real battery capacity *Q* according to Peukert law is lower than the ideal one due to its dependence of dump current intensity and of the power plant required power respectively.

Obtained functional relationship of the eVTOL power plant required power, range, endurance, vertical velocity related to true airspeed as well as eVTOL resultant rotor (wing) trimmed tilt angle in conversion mode are shown on Figure 9-22. Within the airspeed envelope up to 220 km/h, among all wingless eVTOL types, a single rotor helicopter with hybrid power plant has the major range and endurance advantage. Quadcopter with open rotors is the obvious top speed performer with 270 km/h. Within the low speed

envelope up to 60 km/h, ducted fan quadcopter with both hybrid and fully electric power plant has the maximum vertical speed. Ducted fan high efficiency factor at hover and low speed mode explains this feature.

Amongst wingless vehicles with fully electric power plant, quadcopter with open rotors possesses the major range and endurance advantage at speed of 120 km/h. It occurs due to the high relative capacity of its batteries (38.4 % of vehicle mass against 28.5 % of single rotor helicopter).

In addition, it should be noted that quadcopters would have approximately by 50 km/h higher cruising speed compared with single rotor helicopter.

Among the winged eVTOLs, with both fully electric and hybrid power plant, the tiltrotors with ducted fans have the greatest advantages in range and duration of flight. As far as the highest possible performance with the existing electric motors and batteries specific parameters concerns, eVTOL with hybrid power plant will have the best benefit nowadays. Such eVTOLs would have 2 – 2.5 times more range and endurance values as compare as fully electric vehicles.

4. CONCLUSIONS

Based on eVTOL aerodynamic prediction results one may conclude that competitive flight vehicle accommodating up to 4 passengers can be designed as an urban air taxi. It would be possible upon existing today and being emerged in the nearest future technology level.

Fully electrical power plant with batteries as the only power source could be used for the development of wingless eVTOL quadcopter type with cruise flight endurance at about 30 – 40 min and range of 100 – 130 km. The use of winged eVTOL convertible type will increase the range and flight endurance by 50 km and 20 min, respectively. Such performance is quite acceptable for using vehicle as an urban air taxi.

Wingless vehicles with hybrid power plant and 170 – 330 km range would be better employed as intercity transport.

Winged eVTOL with hybrid power plant and 340 – 450 km range are also best suited for long-distance intercity flights.

For skyscraper downtown intracity flights, ducted fan wingless quadcopter eVTOLs will have undoubted advantage due to its high rate of climb.

Among the winged eVTOLs with both fully electric and hybrid power plant, the greatest advantages in range and flight endurance will have aircraft with ducted fans.

Flap system and/or boundary layer active control system is required for tiltwing quadcopter eVTOLs because wings of such vehicles operates at great angles of attack in low airspeed range.

5. SYMBOLS AND ABBREVIATIONS

C_T – rotor thrust coefficient
c_{d_0} – rotor blade drag coefficient
D_{MR} – main rotor diameter
D – VTOL drag
G – VTOL take-off weight
R – rotor radius
m_0 – VTOL take-off mass
m_f – fuel weight (in case of hybrid power plant)
m_{trans} – mechanical transmission mass
$\bar{m}_{\mathrm{FC}}$ – flight control system mass fraction
$\bar{m}_{\mathrm{Ch}}$ – chassis mass fraction
$\bar{m}_{\mathrm{HE}}$ – heat engine mass fraction
$\bar{m}_a$ – airframe mass fraction,
$\bar{m}_{\mathrm{FS}}$ – fuel system mass fraction
$\bar{m}_{\mathrm{OS}}$ – oil system mass fraction
$\bar{m}_{\mathrm{EM}}$ – electric motors mass fraction
$\bar{m}_{\mathrm{GEN}}$ – generators mass fraction
$\bar{m}_{fus}$ – fuselage mass fraction
$\bar{m}_{rs}$ – rotor system mass fraction
$\bar{m}_{TR}$ – tail rotor mass fraction
$\bar{m}_{ae}$ – conventional airborne equipment mass fraction
$\bar{m}_{ue}$ – utility airborne equipment mass fraction
$\bar{m}_{ew}$ – electrical wiring mass fraction
M_0 – rotor tip Mach number in hover mode
$\bar{P}_{\mathrm{EM}}$ – thrust electric motor specific power (main gearbox assembly)
$\bar{P}_{gen}$ – generator specific power
$\bar{m}_{bat}$ – battery mass fraction
$\bar{m}_{inv}$ – invertor mass fraction
$\bar{m}_{EM}$ – electric motors mass fraction

n_{MR} – main rotor number
v – induced velocity
$\bar{P}_{\mathrm{ICE}}$ – heat engine specific power
C_e – specific fuel consumption
P – thrust engine power

P_i – induced power
P_0 – profile loss power
P_w – wave drag power
P_p – parasite drag power
Q – battery capacity, kW·h
T – main rotor thrust
V – eVTOL airspeed
α – rotor angle of attack
α_0 – rotor axis incidence towards wing chord
α_T – flight vehicle trim angle of attack
δ– tilt rotor (wing) deflection angle
μ – rotor advance ratio
λ – inflow ratio
η – main rotors efficiency factor
χ – rotor disk area usability factor
ξ – transmission efficiency factor
ρ – air density
Ω – main rotor angular velocity

6. REFERENCES

1. Myasnikov M.I., Esaulov S.Yu., Ilyin I.R., VTOL Aerodynamic Configurations Analysis for Urban Air Mobility. Presented at the 76th Annual Forum & Technology Display, held online Oct. 5-8, 2020.
2. Myasnikov M.I., Esaulov S.Y., Ilyin I.R. «Light eVTOL Possible Aerodynamic Configurations Analysis». 45th European Rotorcraft Forum, Warsaw, Poland, 17-20 September, 2019.
3. Mil' M.L., Nekrasov A.V., Braverman A.S. Helicopters. Calculation and Design. Volume I. Aerodynamics. Washington: National Aeronautics and Space Administration, 1966.
4. Johnson W. Rotorcraft Aeromechanics. Cambridge University Press, 2013.
5. Shaidakov V.I. Ducted fan aerodynamics. MAI Publishing, 1996.
6. Kundu A.K., Price M.A., Riordan D. Conceptual Aircraft Design: An Industrial Approach. First Edition. John Wiley & Sons, 2019.
7. Gurevich O.S. et al. Electrical rotorcraft. Dvigatel, #2 (80), 2012.
8. Daidzic N. E., Piancastelli L., Cattini A. “Diesel engines for light-to-medium helicopters and airplanes (Editorial)”.International Journal of Aviation, Aeronautics, and Aerospace, Vol. 1 [2014], Iss.3, Art. 2, pp.1-18.

7. FIGURES AND TABLES

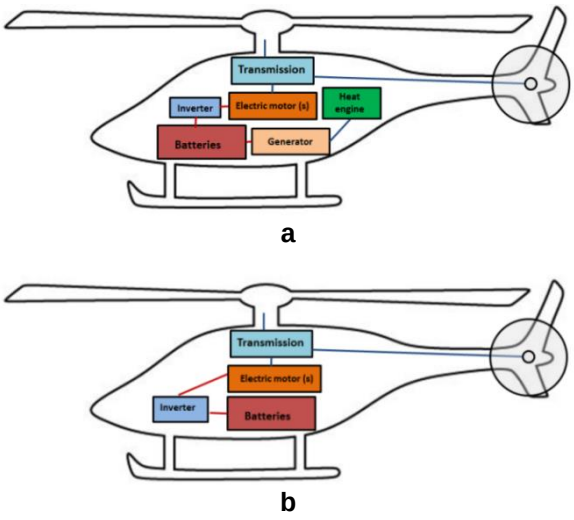

Figure 1. Basic elements of a single-rotor helicopter power plant. Hybrid (**a**) and full-electric (**b**) power plant

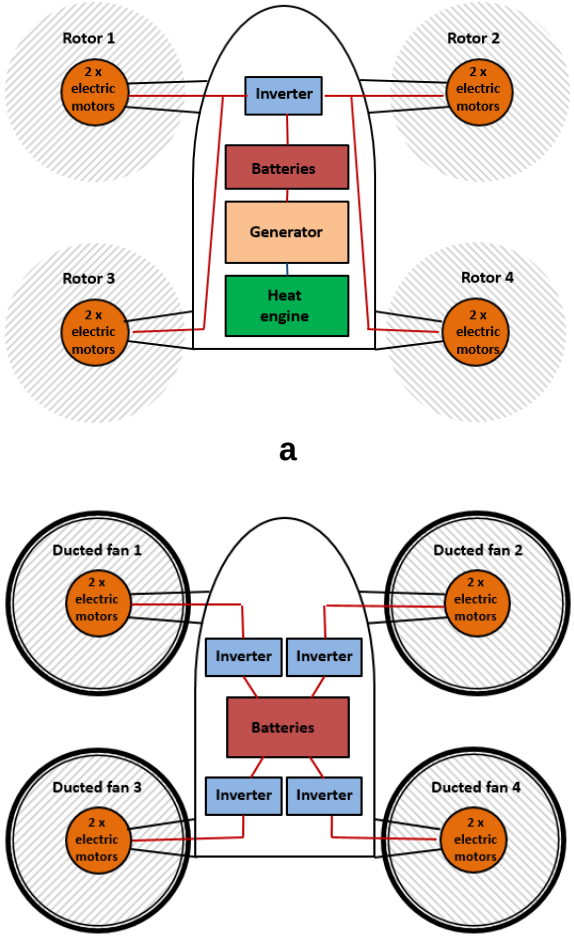

Figure 2. Basic power plant elements of open rotors quadcopter with hybrid power plant (a) and ducted fans quadcopter with fully electric power plant (b)

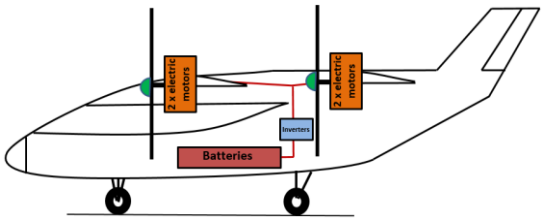

a

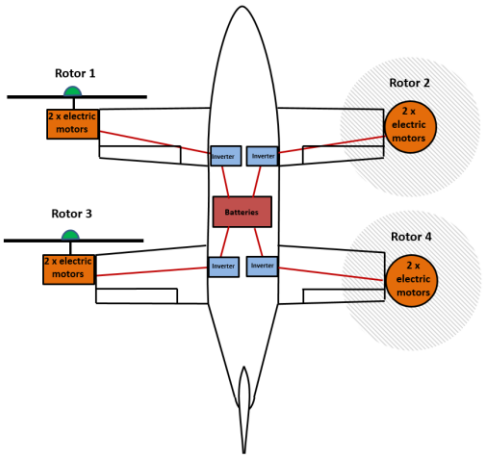

b

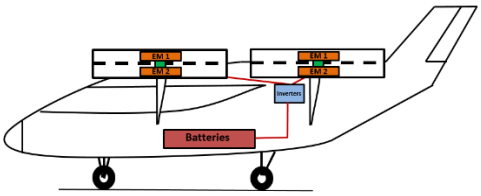

c

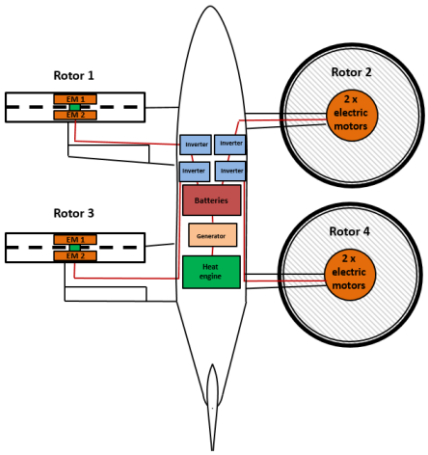

d

Figure 3. Basic elements of tiltrotor (a, b) with open rotors and tiltwing ducted fans (c, d) quadcopters with fully electric (b) and hybrid power plant (d)

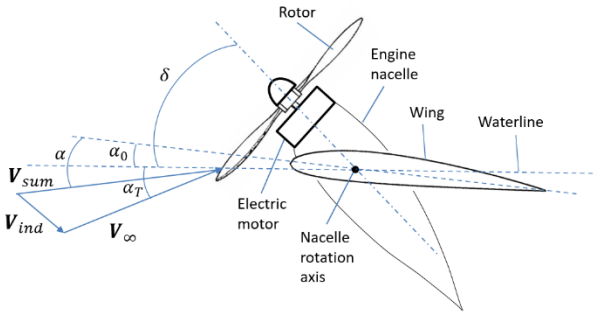

a

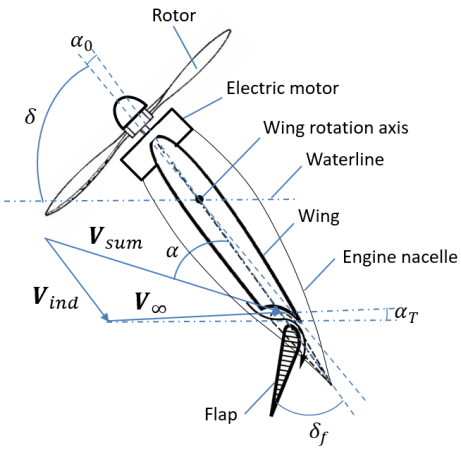

b

Figure 4. Tilted rotor (a) and tilted wing (b) flow scheme. δ – tilt rotor (wing) deflection angle, α_0 – rotor axis incidence towards wing chord, α – rotor angle of attack, α_T – flight vehicle trimmed angle of attack

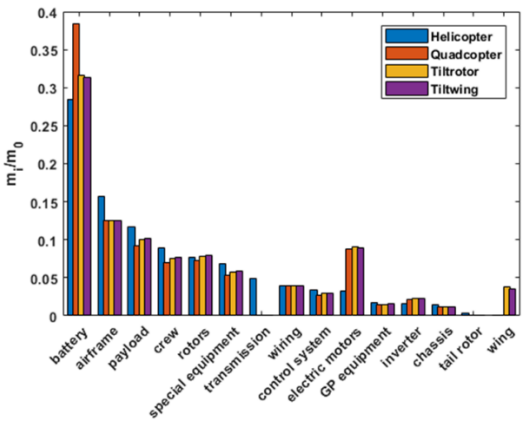

Figure 5. Distribution of structural elements mass for eVTOL with full electric power plant

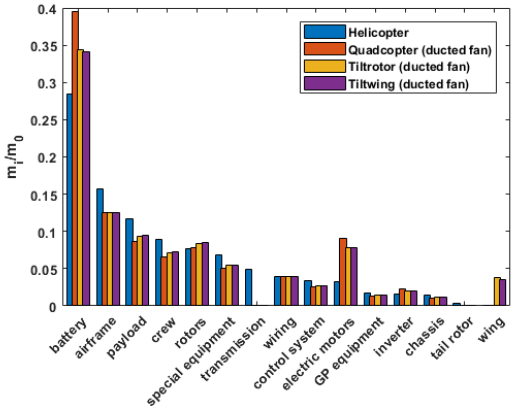

Figure 6. Distribution of structural elements mass for eVTOL with ducted fans and full electric power plant

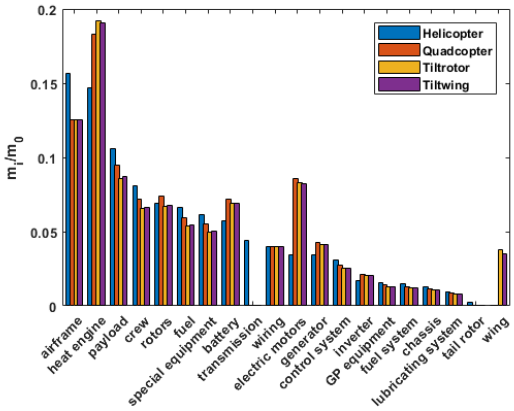

Figure 7. Distribution of structural elements mass for eVTOL with hybrid power plant

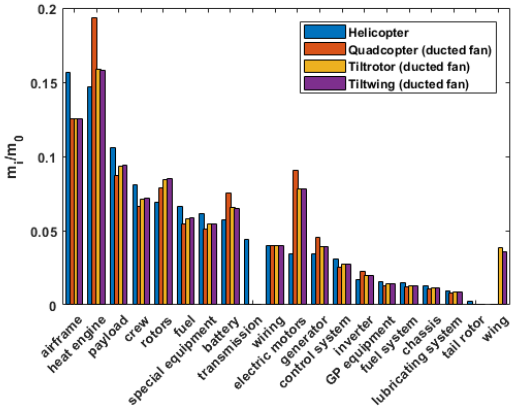

Figure 8. Distribution of structural elements mass for eVTOL with ducted fans and hybrid power plant

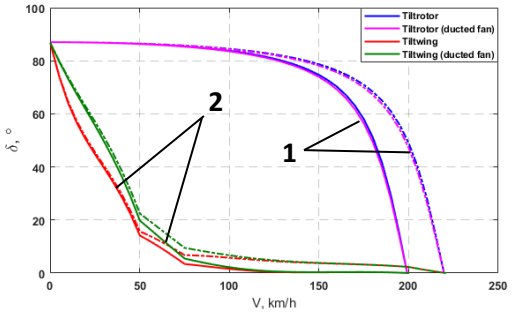

Figure 9. Rotor (wing) trimmed tilt angle calculation for quadcopter eVTOL with tilted rotors (1) and tilted wings (2) in conversion mode. Solid lines - H = 0 m, dashed lines - H = 2000 m. Full electric power plant

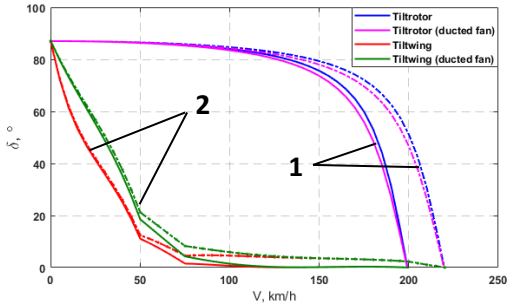

Figure 10. Rotor (wing) trimmed tilt angle calculation for quadcopter eVTOL with tilted rotors (1) and tilted wings (2) in conversion mode. Solid lines - H = 0 m, dashed lines - H = 2000 m. Hybrid power plant

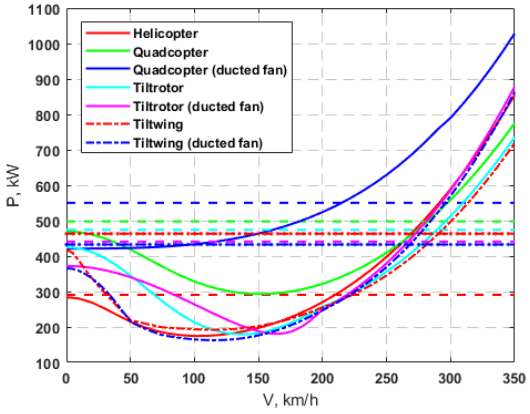

Figure 11. Dependence of the required power of eVTOL on airspeed, H = 0 m. The dashed lines are the available eVTOL power. Full electric power plant

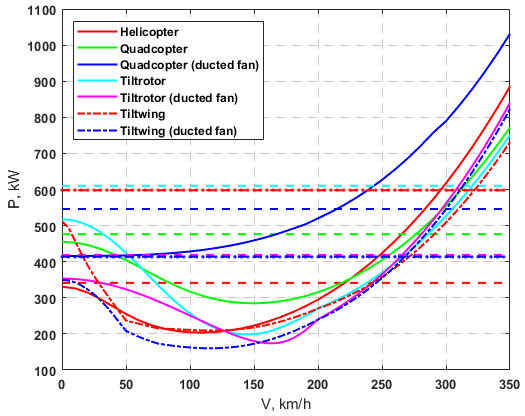

Figure 12. Dependence of the required power of eVTOL on airspeed, H = 0 m. The dashed lines are the available eVTOL power. Hybrid power plant

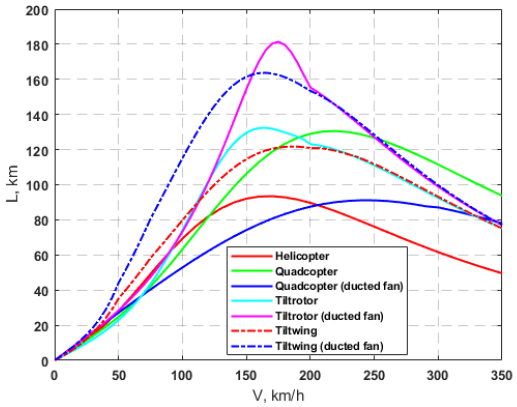

Figure 13. Dependence of the eVTOL flight range on airspeed. H = 0 m. Full electric power plant

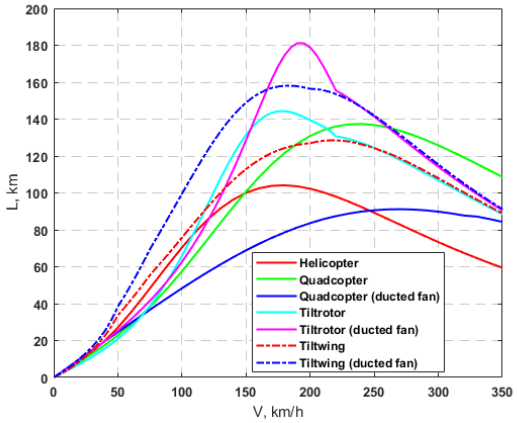

Figure 14. Dependence of the eVTOL flight range on airspeed. H = 2000 m. Full electric power plant

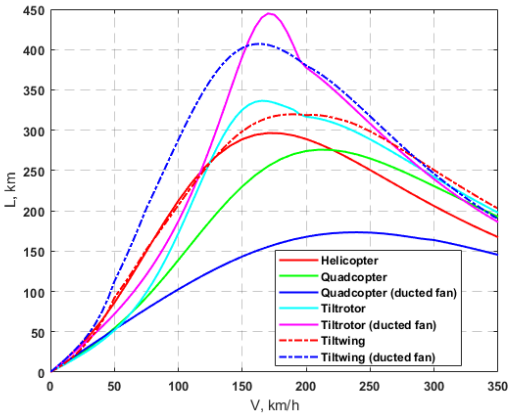

Figure 15. Dependence of the eVTOL flight range on airspeed. H = 0 m. Hybrid power plant

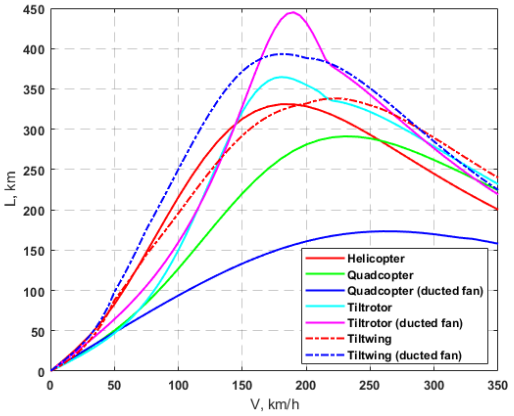

Figure 16. Dependence of the eVTOL flight range on airspeed. H = 2000 m. Hybrid power plant

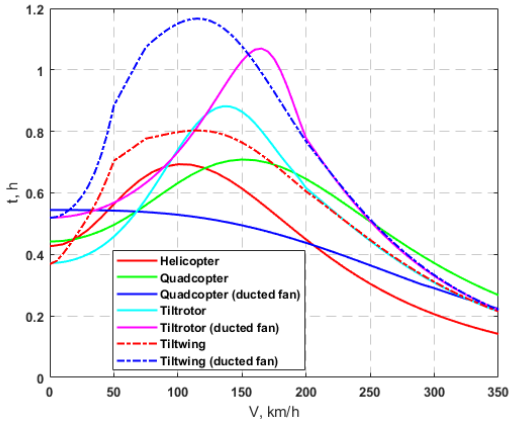

Figure 17. Dependence of the eVTOL flight endurance on airspeed. H=0 m. Full electric power plant

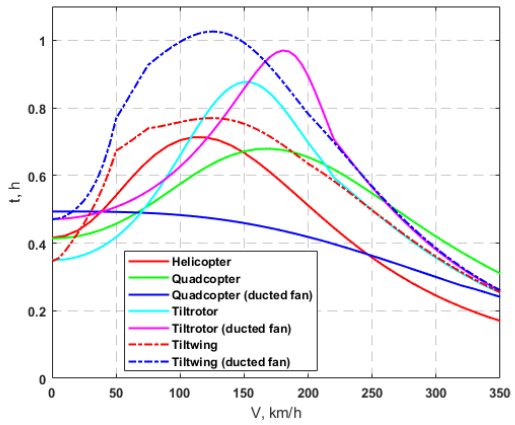

Figure 18. Dependence of the eVTOL flight endurance on airspeed. H=2000 m. Full electric power plant

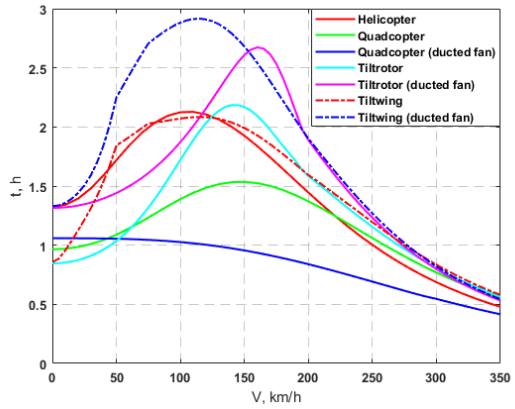

Figure 19. Dependence of the eVTOL flight endurance on airspeed. H=0 m. Hybrid power plant

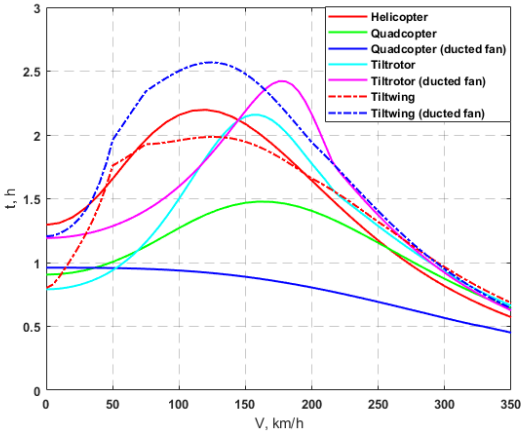

Figure 20. Dependence of the eVTOL flight endurance on airspeed. H=2000 m. Hybrid power plant

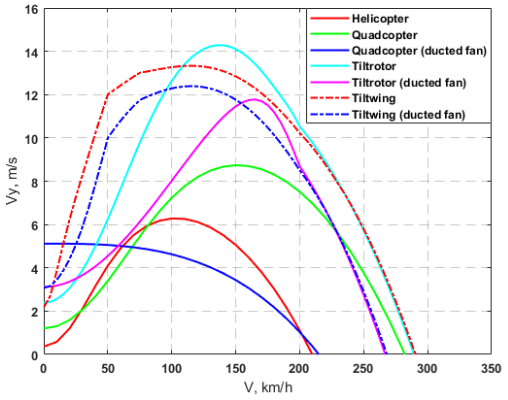

Figure 21. Dependence of the eVTOL vertical velocity on airspeed. H=0 m. Full electric power plant

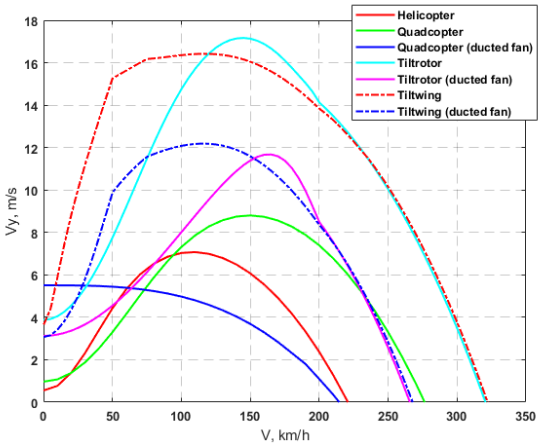

Figure 22. Dependence of the eVTOL vertical velocity on airspeed. H = 0 m. Hybrid power plant

Table 1. Initial data for eVTOL with fully electric power plant performance prediction

Specification	Conventional rotorcraft	Quadcopter with open rotors	Quadcopter with ducted fans	4 X-type tiltrotor vehicle with open rotors and wings	4 X-type tiltrotor vehicle with ducted fans and wings	4 X-type tiltwing vehicle with open rotors and wings	4 X-type tiltwing vehicle with ducted fans and wings
n_{MR}	1	4	4	4	4	4	4
$D_{MR,}$ m	10	3	3	3	3	3	3
η	0.7	0.85	0.9	0.81	0.91	0.81	0.91
χ	0.95	0.95	0.95	0.95	0.95	0.95	0.95
ξ	0.85	1	1	1	1	1	1
$\bar{P}_{EM}$, kW/kg	5	5	5	5	5	5	5
$\bar{m}_{bat}$, kg/kW·h	4	4	4	4	4	4	4
$\bar{m}_{inv}$, kg/kW	0.1	0.1	0.1	0.1	0.1	0.1	0.1
m_{PL}, kg	210	210	210	210	210	210	210
AR	-	-	-	6	6	6	6

Table 2. Initial data for eVTOL with hybrid power plant performance prediction

Specification	Conventional rotorcraft	Quadcopter with open rotors	Quadcopter with ducted fans	4 X-type tiltrotor vehicle with open rotors and wings	4 X-type tiltrotor vehicle with ducted fans and wings	4 X-type tiltwing vehicle with open rotors and wings	4 X-type tiltwing vehicle with ducted fans and wings
n_{MR}	1	4	4	4	4	4	4
$D_{MR,}$ m	10	3	3	3	3	3	3
η	0.7	0.86	0.91	0.79	0.91	0.79	0.91
χ	0.95	0.95	0.95	0.95	0.95	0.95	0.95
ξ	0.85	1	1	1	1	1	1
C_e, kg/kW·h	0.3	0.3	0.3	0.3	0.3	0.3	0.3
$\bar{P}_{EM}$, kW/kg	5	5	5	5	5	5	5
$\bar{P}_{gen}$, kW/kg	5	5	5	5	5	5	5
$\bar{m}_{bat}$, kg/kW·h	4	4	4	4	4	4	4
$\bar{m}_{inv}$, kg/kW	0.1	0.1	0.1	0.1	0.1	0.1	0.1
$\bar{P}_{HE}$, kW/kg	1.3	1.3	1.3	1.3	1.3	1.3	1.3
m_{PL}, kg	210	210	210	210	210	210	210
AR	-	-	-	6	5.6	6	5.6

Presented at 47th European Rotorcraft Forum, United Kingdom, 7-9th September, 2021

Table 3. eVTOL with fully electric power plant predictions

Specification	Conventional rotorcraft	Quadcopter with open rotors	Quadcopter with ducted fans	4 X-type tiltrotor vehicle with open rotors and wings	4 X-type tiltrotor vehicle with ducted fans and wings	4 X-type tiltwing vehicle with open rotors and wings	4 X-type tiltwing vehicle with ducted fans and wings
$\bar{m}_{bat}$	0.2851	0.3844	0.3948	0.3162	0.3435	0.3138	0.3417
$\bar{m}_{rs}$	0.0764	0.0721	0.0775	0.0779	0.0842	0.0791	0.0854
$\bar{m}_{a}$	0.1566	0.1253	0.1253	0.1253	0.1253	0.1253	0.1253
m_{PL}/m_0	0.1174	0.0924	0.0859	0.0998	0.0933	0.1013	0.0945
$\bar{m}_{cr}$	0.0895	0.0704	0.0654	0.0760	0.0711	0.0772	0.0720
$\bar{m}_{ae}$	0.0683	0.0537	0.0499	0.0580	0.0542	0.0589	0.0550
$\bar{m}_{inv}$	0.0163	0.0219	0.0225	0.0225	0.0196	0.0224	0.0195
$\bar{m}_{EM}$	0.0325	0.0876	0.0900	0.0901	0.0783	0.0894	0.0779
$\bar{m}_{FC}$	0.0343	0.0270	0.0251	0.0292	0.0273	0.0296	0.0276
$\bar{m}_{ew}$	0.0400	0.0400	0.0400	0.0400	0.0400	0.0400	0.0400
$\bar{m}_{ue}$	0.0177	0.0139	0.0129	0.0150	0.0141	0.0153	0.0142
$\bar{m}_{Ch}$	0.0144	0.0113	0.0105	0.0122	0.0114	0.0124	0.0116
$\bar{m}_{trans}$	0.0486	0.0000	0.0000	0.0000	0.0000	0.0000	0.0000
$\bar{m}_{TR}$	0.0030	0.0000	0.0000	0.0000	0.0000	0.0000	0.0000
$\bar{m}_{WG}$	0.0000	0.0000	0.0000	0.0377	0.0377	0.0353	0.0353
m_0, kg	1788	2274	2446	2105	2251	2073	2221

Table 4. eVTOL with hybrid power plant predictions

Specification	Conventional rotorcraft	Quadcopter with open rotors	Quadcopter with ducted fans	4 X-type tiltrotor vehicle with open rotors and wings	4 X-type tiltrotor vehicle with ducted fans and wings	4 X-type tiltwing vehicle with open rotors and wings	4 X-type tiltwing vehicle with ducted fans and wings
$\bar{m}_{HE}$	0.1466	0.1830	0.1933	0.1921	0.1586	0.1907	0.1580
$\bar{m}_{a}$	0.1566	0.1253	0.1253	0.1253	0.1253	0.1253	0.1253
m_{PL}/m_0	0.1058	0.0946	0.0872	0.0859	0.0933	0.0870	0.0941
$\bar{m}_{rs}$	0.0688	0.0739	0.0788	0.0670	0.0842	0.0679	0.0850
$\bar{m}_{cr}$	0.0806	0.0721	0.0665	0.0654	0.0711	0.0663	0.0717
$\bar{m}_{bat}$	0.0573	0.0715	0.0756	0.0693	0.0653	0.0689	0.0650
$\bar{m}_{inv}$	0.0172	0.0215	0.0227	0.0208	0.0196	0.0207	0.0195
$\bar{m}_{f}$	0.0660	0.0590	0.0544	0.0536	0.0582	0.0543	0.0587
$\bar{m}_{ae}$	0.0615	0.0550	0.0507	0.0499	0.0542	0.0506	0.0547
$\bar{m}_{EM}$	0.0344	0.0859	0.0907	0.0832	0.0783	0.0826	0.0780
$\bar{m}_{gen}$	0.0344	0.0429	0.0454	0.0416	0.0392	0.0413	0.0390
$\bar{m}_{FC}$	0.0309	0.0277	0.0255	0.0251	0.0273	0.0254	0.0275
$\bar{m}_{ew}$	0.0400	0.0400	0.0400	0.0400	0.0400	0.0400	0.0400
$\bar{m}_{ae}$	0.0160	0.0143	0.0131	0.0129	0.0141	0.0131	0.0142
$\bar{m}_{fs}$	0.0147	0.0132	0.0121	0.0119	0.0130	0.0121	0.0131
$\bar{m}_{Ch}$	0.0130	0.0116	0.0107	0.0105	0.0114	0.0107	0.0115
$\bar{m}_{os}$	0.0096	0.0086	0.0079	0.0078	0.0085	0.0079	0.0085
$\bar{m}_{trans}$	0.0438	0.0000	0.0000	0.0000	0.0000	0.0000	0.0000
$\bar{m}_{TR}$	0.0027	0.0000	0.0000	0.0000	0.0000	0.0000	0.0000
$\bar{m}_{WG}$	0.0000	0.0000	0.0000	0.0377	0.0385	0.0351	0.0360
m_0, kg	1984	2219	2407	2446	2251	2413	2231